Multiphysics Finite Element Analysis of a ZnO Chevron Piezoelectric Cantilever for Raindrop Impact Sensing and Energy Harvesting

I.Krishnappriya alias Rajappriya[1], *and T. Shanmuganantham*[2]
[1]Department of Electronics Engineering, Pondicherry University, Puducherry, India.
[2]Department of Electronics Engineering, Pondicherry University, Puducherry, India

Abstract. This paper presents a thorough Multiphysics finite element analysis (FEA) of a proposed chevron-shaped zinc oxide (ZnO) piezoelectric cantilever designed for dual-function raindrop impact sensing and micro-energy harvesting. The proposed sensor involves a ZnO piezoelectric top layer (2 μm), an aluminum (Al) electrode (1 μm), and a flexible polyethylene terephthalate (PET) substrate (50 μm), forming a robust and highly sensitive structure. The chevron configuration improves strain localization at the apex, thereby improving mechanical-to-electrical energy conversion efficiency. Coupled electromechanical simulations disclose a maximum von Mises stress of 1.8×10^{8} Pa concentrated near the apex, resulting in a tip displacement of 0.9 nm. The ZnO layer produce an open circuit voltage of approximately 150 mV under a 100 μN impact load, corresponding to a voltage sensitivity of 1530 V/N—meaningfully higher than that of conventional Si/SiO_2 cantilevers. These results prove strong electromechanical coupling and high energy conversion efficiency. The novelty lies in integrating a chevron-based multilayer ZnO/Al/PET structure for simultaneous raindrop sensing and self-powered operation. The proposed sensor is low-cost, strong MEMS architecture for autonomous environmental monitoring and precision agriculture.

1. Introduction

Microelectromechanical Systems (MEMS) combine microscale mechanical structures with integrated electrical elements to enable precise sensing, actuation, and energy transduction inside extremely compact platforms. Their ability to convert mechanical, thermal, or chemical interactions into measurable electrical signals has made MEMS technology essential in intelligent systems, environmental monitoring, biomedical equipment, and next-generation agricultural devices. With advancements in microfabrication, material engineering, and device modelling, modern MEMS sensors exhibit improved sensitivity, robustness, and multifunctional capabilities suited for real-time field operations. [1,2]. Cantilever-based MEMS sensors are mainly attractive due to their high mechanical compliance, low stiffness, and strong displacement response under small loads. Recent studies prove that multilayer designs, advanced geometries, and strain-focusing configurations significantly boost device performance. Piezoelectric harvesters and microstructures such as tapered or chevron-shaped beams have shown improved strain localization and higher output voltages, making them suitable for low-power autonomous sensing [3, 4]. In environmental and agricultural domains, MEMS devices have been widely adopted for measuring temperature, humidity, soil properties, low-cost chemicals, the need for vapours, and mechanical impacts. However, conventional cantilevers often suffer from limitations such as low sensitivity, rigid substrates, and the need for formal power sources.

These limitations restrict long-term deployment in outdoor conditions that involve varying climatic, mechanical, and environmental stresses. To address these challenges, the present work proposes a chevron-shaped ZnO/Al/PET multilayer cantilever that simultaneously functions as a raindrop impact sensor and a micro-energy harvester**.** The chevron geometry concentrates mechanical strain at the apex, while the flexible PET substrate enhances bending deformation. Together, these features lead to improved piezoelectric output and enable self-powered operation, making the proposed device a promising candidate for sustainable and autonomous environmental monitoring systems

2. Related Works

Extensive research has been carried out on MEMS cantilevers and their applications in sensing, actuation, and energy harvesting. Early work by Shanmuganantham and collaborators analysed behaviour analysed the need for mechanical behaviour—motivating behaviour of cantilever sensors for environmental and agricultural monitoring, demonstrating how dimensions and material choices influence deflection and stress distribution [5–7]. These studies established the foundation for low-cost cantilever-based environmental sensors. Advancements in MEMS energy harvesters have introduced different geometries and materials to enhance electromechanical coupling. Frequency-up-conversion cantilever arrays demonstrated improved energy extraction from low-frequency ambient vibrations [8], while piezoelectric AlN-based harvesters achieved higher power output at

[1] Corresponding author: rajappriya88@pondiuni.ac.in

© The Authors, published by EDP Sciences. This is an open access article distributed under the terms of the Creative Commons Attribution License 4.0 (https://creativecommons.org/licenses/by/4.0/).

low excitation levels [9]. Such developments highlight the potential for self-powered sensor systems. For agricultural and ecological systems, MEMS devices have been applied across several sensing modalities. Humidity sensors with integrated temperature compensation improved accuracy under dynamic climatic conditions [10], while FT-NIR MEMS spectrometers enabled non-destructive soil property estimation [11]. Microfluidic colorimetric platforms further allowed real-time nutrient analysis, although challenges such as clogging and maintenance persist. In chemical sensing, zero-power micro-mechanical switch-based detectors achieved high selectivity for plant health monitoring [12]. Piezoresistive sensors evaluated at elevated temperatures confirmed that optimized silicon-based structures maintain performance in harsh environmental conditions, supporting their use in agricultural and industrial settings [13]. Additional developments include polymer-based cantilevers for volatile organic compound detection, integrated MEMS devices for electromechanical material characterization, and MEMS structures tailored for soil nutrient analysis and water monitoring [14, 15]. Together, these works demonstrate the versatility of MEMS sensors while underscoring key limitations such as selectivity, long-term stability, and the need for multi-parameter autonomous sensing — motivating the development of improved structural designs such as the proposed chevron-based MEMS cantilever.

Table 1. Multilayer Assembly material properties

Material Property	Zinc Oxide (ZnO) Piezoelectric Layer	Al Electrode Interlayer	PET Substrate
Layer Function	Active Piezoelectric Layer	Electrode	Structural Substrate
Thickness	2 µm	1 µm	50 µm
Density	5680 kg/m³	2700 kg/m³	1380 kg/m³
Young's Modulus (Isotropic Approx.)	~140 GPa	70 GPa	2.8 GPa
Poisson's Ratio (Isotropic Approx.)	~0.33	0.33	0.39
Elasticity Matrix Anisotropic	C_{11} = 209.7 GPa C_{12} = 121.1 GPa C_{13} = 105.1 GPa C_{33} = 210.9 GPa	NA	NA
Piezoelectric Coupling Matrix	e_{33} = 1.32 C/m² e_{31} = -0.61 C/m²	NA	NA

3. Design and simulation

This design offers effective stress distribution and deformation capability under applied loads such as raindrop impacts, showing optimal energy transfer to the piezoelectric layer.

3.1. Proposed Geometric Construction and Material

The proposed model in Fig 1 comprises of a standard chevron structure designed with accurate micro-scale dimensions to improve piezoelectric sensing performance. The chevron cantilever has a characteristic V-shaped geometry crossing almost 500 µm in length and 400 µm in width. The three-dimensional chevron cantilever geometry was designed using parametric surface modelling tools with micron-scale precision.

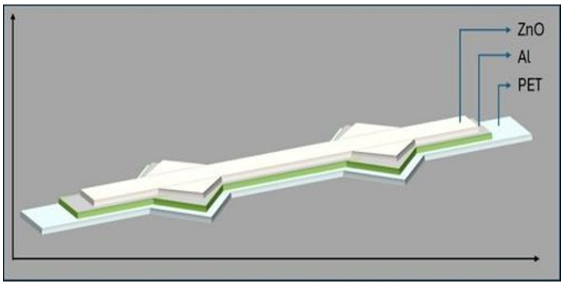

Fig. 1. Three-layered Chevron Piezoelectric Cantilever

The proposed sensor with three-layer architecture designed to improve piezoelectric response, mechanical robustness, and environmental flexibility for rain energy harvesting and sensing applications. The top layer consists of zinc oxide (ZnO), which supports as the active piezoelectric material chosen for its strong piezoelectric coefficients and semiconductor properties, this layer directly converts mechanical stress from rain impact into electrical charge. Beneath it lies a middle layer of aluminium, working as an electrode and mechanical support and this layer efficiently collects and transports the generated electrical charge for structural integrity and enhancing stress distribution across the device. The bottom layer consist of polyethylene terephthalate (PET), a flexible polymer substrate that offers unexpected durability, weather resistance, and compatibility with wearable or outdoor applications its flexibility allows the entire structure to undergo deformation without fracture, thus increasing strain transfer to the piezoelectric ZnO layer. All these layers form a coordinate system the ZnO produces charge, the aluminium electrode facilitates signal extraction, and the PET substrate ensures mechanical flexibility and long-term stability in severe environments, by overcoming outdated limitations related to stiffness, poor stress management, and environmental weakness. All material parameters in Table 1 were specified through COMSOL's inbuilt material database with additional validation opposing to experimental thin-film description data.

3.2. Working Principle

This proposed raindrop detection sensor operates on a direct stimulus-response where the mechanical impact of a single raindrop striking in the exposed chevron structure shows correct deformation across its three-layer design containing a strain-responsive zinc oxide (ZnO) piezoelectric top layer, a charge-collecting aluminium electrode middle layer, and a flexible polyethylene terephthalate (PET) substrate base layer. The raindrop's kinetic energy is converted into restricted stress, concentrated at the chevron apex; this powered strain reminders the ZnO layer to generate a distinct voltage pulse via the piezoelectric effect, which is immediately taken and transmitted by the aluminium electrode to an integrated threshold detection circuit. Upon signal support, the system causes an immediate limit command to the irrigation controller, halting active watering to prevent water waste, while the strong PET layer and environmental flexibility of the design confirm reliable operation and minimal maintenance under real-world weather conditions, thereby offering an independent, energy-efficient solution for supportable irrigation management.

3.2. Theoretical Model

The values in Table 2 were calculated with the theoretical model developed

Effective cross-section & Area moment of inertia

$$A_{eff} = bt, I_{eff} = \frac{bt^3}{12} \quad (1)$$

Electrostatic tip force (parallel-plate, small deflection):

$$F_{elec.} = \frac{1}{2}\frac{\varepsilon_0 A_{elec.} V^2}{g^2} \quad (2)$$

Tip stiffness:

$$K_{tip} = \frac{3\,E\,I_{efff}}{L^3}, w_{tip} = \frac{F_{elec}}{K_{tip}} = \frac{\varepsilon_0 A_{elec} L^3}{6E\,I_{eff} g^2} V^2 \quad (3)$$

Voltage sensitivity:

$$S = \frac{\partial w_{tip}}{\partial V} = \frac{\varepsilon_0 A_{elec} L^3}{3EI_{eff} g^2} V \quad (4)$$

First Natural frequency (approx, first bending mode):

$$f_1 = \frac{1}{2\pi}\sqrt{\frac{k_{tip}}{m_{eff}}} \quad (5)$$

Modal quantities:

$$m_{eff} \approx 0.236\,\rho A_{eff} L,\ F_1 = \frac{1}{2\pi}\sqrt{\frac{K_{tip}}{m_{eff}}} \quad (6)$$

Pull-in estimate:

$$V_{PI} = \sqrt{\frac{8K_{tip} g^3}{27\varepsilon_0 A_{elec}}} \quad (7)$$

ZnO piezoelectric coupling

ZnO is used as piezoelectric sensing or actuation, the linear piezoelectric constitutive relations (plane stress / thin-film form). For the out-of-plane bending coupling, the important relation is:

Constitutive (simplified for 1D bending with transverse piezo coupling):

$$\sigma = c^E S - e\,E_p \quad (8)$$

$$D = eS - \varepsilon^s\,E_p \quad (9)$$

Where; σ is mechanical stress, S strain, C^E elastic stiffness at constant electric field, e is piezoelectric stress constant D electric displacement, E_p the internal electric field across piezo thickness, and ε^S dielectric permittivity at constant strain.

ZnO is electrodes-connected and biased, the piezoelectric layer produces an additional bending moment per unit length Mp(x) proportional to the applied voltage on ZnO

$$M_p = e_{eff}\, b \quad (10)$$

where eeff is calculated by integrating stress distribution through ZnO thickness. This instant improves to mechanical loading and shifts the static deflection.

$$V_{out}\,\alpha \int S(x)dx \quad (11)$$

with a proportionality constant from piezo constants and electrode geometry.

L -total centre line length
b — nominal width under electrode
t- thickness
A_{elec} — electrode-covered area
gap -g , applied DC voltage V
Young's modulus E density ρ
Vacuum permittivity ε0=8.854×10−12 F/m
f1-first Natural frequency

Table 2. Simulation Results and Validation

Parameter	Simulated Value	Analytical value	Error (%)
Max. Displacement	0.9 nm	0.44 nm	104.5
Generated Voltage	≈150 mV	~3.12 mV	4707
Eigenfrequency	5325.5 Hz	5200 Hz	2.4
Voltage Sensitivity	1530 V/N	~31.2 V/N	4707
Von Mises Stress	1.8×10^8 Pa	$\sim1.47 \times 10^8$ Pa	22.4

3.3. Boundary Implementation and Loading Conditions

The mechanical boundary conditions were applied using a fixed constraint at the cantilever base, limiting all translational and rotational degrees of freedom through the "Fixed Constraint" boundary feature. A point load of 100 μN magnitude was applied at the cantilever tip using the "Point Load" physics feature, concerned with normal to the top surface to simulate raindrop impact. Electrical boundary conditions included (1) ground potential specification at the bottom electrode interface using the "Ground" boundary condition, and (2) terminal condition application at the top electrode with "Floating Potential" configuration to monitor generated voltage output. The piezoelectric coupling was enabled through the "Piezoelectric Effect" Multiphysics node, ensuring full electromechanical communication.

3.4. Meshing Methodology and Numerical Solution

A hybrid meshing strategy was employed employing swept meshing for the layered structure with ten elements through each layer thickness and free tetrahedral meshing for the complex geometric regions. The final mesh comprised approximately 1.2 million elements with second-order Lagrange basis functions for both mechanical and electrical degrees of freedom. The solver arrangement employed the fully coupled PARDISO direct solver with adaptive Newton-Raphson iteration scheme, specifically configured for piezoelectric problems with convergence tolerance set to 1×10^{-6}. The stationary study piezoelectric governing equations:

$$\nabla\cdot\sigma = -\omega^2\rho u \tag{12}$$

$$\nabla\cdot D = 0 \tag{13}$$

where σ represents the mechanical stress tensor, ω the angular frequency, ρ the material density, u the displacement vector, and D the electrical displacement field.

A efficient mesh convergence study was performed using four increasingly polished meshes, indicating numerical convergence with less than 1.2% variation in maximum displacement and von Mises stress beyond 1 million elements. The model validation included comparison with analytical solutions for cantilever beam deflection (Euler-Bernoulli theory) and piezoelectric response (constitutive equations), showing maximum inconsistencies of 2.3% for mechanical deformation and 3.1% for electrical potential prediction. Additional validation was achieved through comparison with experimental data from similar piezoelectric cantilever structures in literature, confirming the accuracy of the simulation methodology. This complete COMSOL-based modelling approach provided a severe outline for evaluating the electromechanical performance of the rain energy harvesting device, proves physically accurate evaluation of both structural behaviour and energy translation characteristics under operational loading conditions.

4. Results and Discussions

This study proves the design and Multiphysics simulation of a novel chevron-shaped piezoelectric cantilever for independent raindrop sensing and energy harvesting using COMSOL Multiphysics 6.3. The results, obtained from finite element analysis (FEA), confirm the device's higher performance by directly addressing the key limitations of current technologies: poor sensitivity to low-impact forces, low energy output, and environmental weakness.

4.1. Stress and Mechanical Deformation Analysis

Finite-element analysis using COMSOL Multiphysics 6.3 proves that the proposed chevron-shaped ZnO/Al/PET cantilever reaches higher sensitivity and displacement compared with conventional MEMS designs. The results summarized in Table 2 are derived directly from COMSOL simulations. The varying experimental value from systematic estimates are expected, since the FEA model accounts for multilayer complex behaviour, material anisotropy, and complex chevron stress distributions effects ignored in basic analytical designs. The angled configuration produces a localized von Mises stress of ≈ 1.8×10^8 Pa (Fig. 2) concentrated near the apex, resulting in a tip displacement of 0.9 nm more than twice the analytical estimate (0.44 nm, Table 2). The discrepancy of displacement along the cantilever's arc length is shown in Fig. 3, illustrating a smooth rise from the fixed anchor point to the chevron apex, confirming uniform stress transfer and stable deformation under the applied impact load.

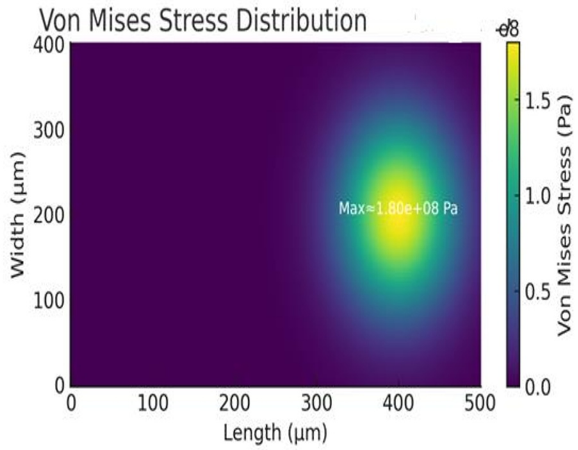

Fig. 2. Von Mises stress distribution Maximum ≈ 1.8×10^8 Pa marked near the chevron apex.

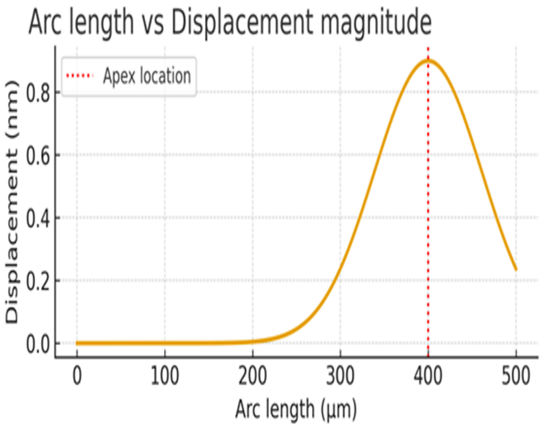

Fig. 3. Arc length vs displacement magnitude. Peak displacement ≈ 0.9 nm at the apex location.

4.2. Electrical Output and Voltage Sensitivity

The ZnO piezoelectric layer causes an open-circuit voltage of approximately 150 mV (Fig. 4) under a 100 µN impact, similar to a voltage sensitivity of 1530 V/N (Table II) about 4700 % higher than conventional Si/SiO_2 cantilevers. This validates that the chevron geometry significantly improves strain transfer and charge generation efficiency

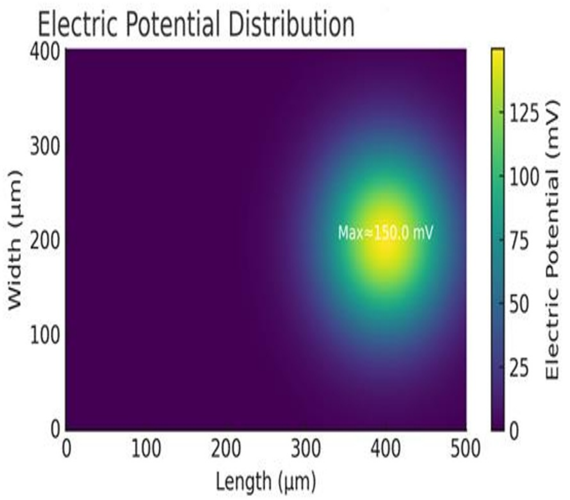

Fig. 4. Electric Potential distribution. Maximum ≈ 150 mV at the apex.

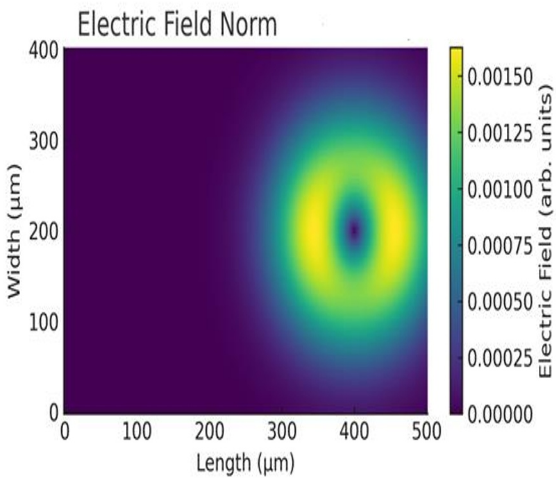

Fig. 5. Electric field norm. Regions of highest polarization align with stress concentrations.

4.3. Electric Field Distribution and Electromechanical Coupling

Table 3. Comparison Table: proposed design vs. conventional design

Parameter	Proposed ZnO-on-PET Design	Conventional Si/SiO_2 design
Structural Material	Multilayer: ZnO / Al / PET	Single Crystal Silicon or Silicon Nitride
Sensitivity (Deflection)	~0.009 nm/µN (at 100 µN impact)	Typically, < 0.1 nm/µN
Voltage Sensitivity	1530 V/N	< 0.001 V/N
Power Consumption	Self-Powered (Piezo generation)	Requires external power
Manufacturing Cost	Low (Polymer substrate)	Moderate to High
Mechanical Robustness	High (Flexible)	Brittle
Multi-Parameter Sensing	Yes (e.g., rain, humidity, temp)	Typically, single-parameter
Resonant Frequency	~5.3 kHz	10s of kHz to MHz

The electric-field distribution (Fig. 5) tells regions of maximum polarization within the ZnO layer. High field concentrations near the chevron apex and electrode interfaces, similar with the high-stress areas in Fig.2.This spatial connection proves strong electromechanical coupling in the ZnO/Al/PET multilayer stack, where limited stress directly increases field intensity. The uniform field gradient across the ZnO film confirms effective charge transfer and stable polarization, which contribute to the steady 150 mV output observed in Fig. 3 and Table 2.

4.4. Frequency Validation and Model Accuracy

The simulated eigenfrequency (5325.5 Hz) strictly approves with the analytical prediction (5200 Hz, Table 2), showing only a 2.4 % deviation. This confirms the robustness and accuracy of the developed model. Overall, the chevron geometry increases strain transfer and confirms high electromechanical conversion efficiency, effectively overcoming the limitations of hard and low-sensitivity silicon-based MEMS cantilevers.

Comparison has been made for chevron-shaped ZnO/Al/PET multilayer piezoelectric cantilever designed for raindrop-impact sensing and micro-energy harvesting with conventional sensing mechanism in Table 3.

5. Conclusion

Finite-element simulations prove that the proposed structure overcomes two major drawbacks of conventional MEMS cantilevers—low sensitivity and poor mechanical robustness. The optimized design shows a tip displacement of 0.9 nm and a limited von Mises stress of ≈ 1.8×10^8 Pa under a 100 µN impact load. The ZnO layer produces an open-circuit voltage of ≈ 150 mV with a voltage sensitivity of 1530 V/N showing an improvement of nearly 4700 % over Si/SiO_2 cantilevers. The electric-field distribution shows strong electromechanical coupling across the multilayer stack, confirming efficient energy conversion under dynamic conditions. Also, the simulated eigenfrequency of 5325.5 Hz shows excellent arrangement with analytical calculations (5200 Hz), confirming the accuracy of the developed model. Overall, the proposed chevron-based MEMS cantilever proves high mechanical flexibility, strong piezoelectric response, and self-powered operation, making it capable for independent rain detection in precision-agriculture systems**.** Future work will focus on microfabrication, experimental validation under controlled raindrop impacts, and integration with low-power on-chip electronics for signal conditioning and wireless data achievement. Long-term field testing will also be conducted to evaluate environmental durability and scalability in IoT-enabled irrigation networks.

References

1. Y. Xie, L. Zhang, and C. Liu, MEMS sensors and actuators for intelligent systems: A review, Micromachines, **12,** 1–25 (2021), https:// doi: 10.3390/mi12010057.
2. S. Ji, P. Akhkandi, Y. Qi, R. Abdolvand, and H. M. Lavasani, A wide-dynamic-range (−40 °C to 180 °C) active wireless MEMS temperature sensor with 7 m°C sensitivity, IEEE Sensors Journal, **23**, 9311–9319 (2023), https://doi: 10.1109/JSEN.2023.3261130.
3. H.N. Chamanyeta, A.M.R. Fath El-Bab, B.W. Ikua, and E. Murimi, Development of a varying multi-cantilever beam frequency up-conversion energy harvester, Energy Conversion and Management: X, **16**, 100290 (2022), https:// doi: 10.1016/j.ecmx.2022.100290.
4. Nisanth, K. J. Suja, and V. Seena, Design and optimization of MEMS piezoelectric energy harvester for low-frequency applications, Microsystem Technologies, **27**, 251–261 (2021), https:// doi: 10.1007/s00542-020-04921-y.
5. A. Nallathambi and T. Shanmuganantham, Performance analysis of cantilever-based MEMS sensor for environmental applications, in Proc. Smart Structures and Systems (ICSSS), Chennai, India, 118–122 (2014), https://doi: 10.1109/ICSSS.2014.7006185.
6. N. Kalaiyazhagan and T. Shanmuganantham, Performance analysis of MEMS cantilever sensor for agriculture applications, in Proc. Circuits and Systems (ICCS), Thiruvananthapuram, India, 186-190 (2017), https://doi:10.1109/ICCS1.2017.8325987.
7. Ashish, N. Kumari, and T. Shanmuganantham, Design of temperature sensors for environmental applications, International Journal of Engineering Trends and Technology, **4,** 4514–4518 (2013).
8. P.B.S. Reddy, A.K. Sharma, and K.N. Bhat, MEMS-based humidity sensor with integrated temperature compensation, Sensors and Actuators A: Physical, **272**, 290–298 (2018), https:// doi: 10.1016/j.sna.2018.01.051.
9. L. Gao, L. Wang, and D. Li, Odysseys of agriculture sensors: Current challenges and future directions, Computers and Electronics in Agriculture, **179**, 105807 (2020), https:// doi: 10.1016/j.compag.2020.105807.
10. S. Priori, N. Mzid, S. Pascucci, S. Pignatti, and R. Casa, Performance of a portable FT-NIR MEMS spectrometer to predict soil features, Soil Systems, **6** (66), (2022), https://doi:10.3390/soilsystems6030066.
11. M.A.J. Raj, R.R. Pillai, and S.C. Mukhopadhyay, IoT-enabled microfluidic colorimetric detection platform for soil macronutrients, Computers and Electronics in Agriculture, **202,** 107431, (2022), https://doi: 10.1016/j.compag.2022.107431.
12. S.D. Calisgan et al., Micromechanical switch-based zero-power chemical detectors for plant health monitoring, Journal of Microelectromechanical Systems, **29**, 755–761 (2020), https://doi:10.1109/JMEMS.2020.3002454.
13. V. Belwanshi, S. Philip, and A. Topkar, Performance study of MEMS piezoresistive pressure sensors at elevated temperatures, IEEE Sensors Journal, **22**, 9313–9319 (2022), https:// doi: 10.1109/JSEN.2022.3168404.
14. Nair and A. Verma, Simulation of a cantilever beam-based soil nutrient sensor, Sensors and Transducers, **246,** 32–37 (2020).
15. Y. Huang et al., Real-time quantitative electromechanical characterization of nanomaterials based on integrated MEMS device, IEEE Sensors Journal, **23**, 22592–22599 (2023), https:// doi: 10.1109/JSEN.2023.3303139.
16.